Pharm Res (2012) 29:806–817
DOI 10.1007/s11095-011-0605-4

RESEARCH PAPER

Improving the Chemical Stability of Amorphous Solid Dispersion with Cocrystal Technique by Hot Melt Extrusion

Xu Liu • Ming Lu • Zhefei Guo • Lin Huang • Xin Feng • Chuanbin Wu

Received: 8 June 2011 / Accepted: 29 September 2011 / Published online: 19 October 2011

ABSTRACT

Purpose To explore *in-situ* forming cocrystal as a single-step, efficient method to significantly depress the processing temperature and thus minimize the thermal degradation of heat-sensitive drug in preparation of solid dispersions by melting method (MM) and hot melt extrusion (HME).

Methods Carbamazepine (CBZ)-nicotinamide (NIC) cocrystal solid dispersions were prepared with polymer carriers PVP/VA, SOLUPLUS and HPMC by MM and/or HME. The formation of cocrystal was investigated by differential scanning calorimetry and hot stage polarized optical microscopy. State of CBZ in solid dispersion was characterized by X-ray powder diffraction and optical microscopy. Interactions between CBZ, NIC and polymers were investigated by FTIR. Dissolution behaviors of solid dispersions were compared with that of pure CBZ.

Results CBZ-NIC cocrystal with melting point of 160°C was formed in polymer carriers during heating process, and the preparation temperature of amorphous CBZ solid dispersion was therefore depressed to 160°C. The dissolution rate of CBZ-NIC cocrystal solid dispersion was significantly increased.

Conclusions By *in-situ* forming cocrystal, chemically stable amorphous solid dispersions were prepared by MM and HME at a depressed processing temperature. This method provides an attractive opportunity for HME of heat-sensitive drugs.

KEY WORDS carbamazepine · cocrystal · hot melt extrusion · solid dispersion · thermal degradation

X. Liu • M. Lu (✉) • Z. Guo • L. Huang • X. Feng • C. Wu (✉)
School of Pharmaceutical Sciences, Sun Yat-Sen University
Guangzhou 510006 Guangdong, People's Republic of China
e-mail: loment.lu@yahoo.com.cn
e-mail: Cbwu2000@yahoo.com

C. Wu
Research & Development Center of Pharmaceutical Engineering
Sun Yat-Sen University
Guangzhou 510006, People's Republic of China

ABBREVIATIONS

CBZ	carbamazepine
DSC	differential scanning calorimetry
FTIR	fourier transform infrared spectroscopy
HME	hot melt extrusion
HPLC	high performance liquid chromatography
HSPM	hot stage polarized optical microscopy
MM	melting method
NIC	nicotinamide
T_g	glass transition temperature
T_m	melting point
TGA	thermal gravimetric analysis
XRPD	X-ray powder diffraction

INTRODUCTION

Solid dispersion is one of the most effective approaches to improve dissolution rate and hence bioavailability of poorly water-soluble drugs (1,2). However, a major limitation of solid dispersion is that amorphous drug is thermodynamically unstable and apt to recrystallize during storage, especially when trace amount of crystalline drug is left in solid dispersion which will act as nucleating agents to accelerate recrystallization of amorphous drug substance (3,4). Therefore, complete transformation of crystalline drug to amorphous state is the key point to improve physical stability and dissolution performance of the solid dispersion.

Recently, melting method (MM) and hot melt extrusion (HME) have gained popularity for preparing solid dispersion due to many advantages, such as free of solvents, simple procedures and uniform product quality (5,6). For both methods, the melting temperature must be high enough to ensure that the drug is completely melted and transformed to amorphous state. But at high temperature,

both drug and polymer carriers face the risk of thermal degradation, especially for heat sensitive drugs (7,8). Therefore, how to decrease the processing temperature of MM and HME is a big challenge for pharmaceutical scientists. Adding plasticizer was a traditional method to depress the glass transition temperature (T_g) and viscosity of polymer carrier to improve processability at lower temperature (9,10). But plasticizer can't change the melting point (T_m) of drug. Lakshman (3) reported a new method that heat-sensitive drug was firstly converted to an amorphous form by spray drying and then melt-extruded with polymer. By this means, melt extrusion was performed below the T_m of drug to effectively avoid thermal degradation. However, this method possessed many disadvantages, such as high preparation cost, solvent residue and environmental pollution.

Cocrystallization was one of the most popular solid state approaches to modify the physicochemical properties of drug such as melting point, solubility and physical stability, without compromising its structural integrity and bioactivity. A cocrystal can be defined as a single crystalline homogenous phase consisting of multiple neutral components which are solid in their pure forms under ambient conditions (11). The components in a cocrystal exist in a definite stoichiometric ration and assemble via noncovalent interactions such as hydrogen bonds, π-π packing, and van der Waals interactions. Schultheiss (11) analyzed the melting points of 50 cocrystalline samples and found that 51% cocrystals had moderate T_m between T_ms of drug and coformer, while 39% have lower T_m than T_ms of drug and coformer. Therefore, cocrystallizing drug with proper coformer may be considered as a good approach to decrease the T_m of drug and minimize the thermal degradation. There are two methods to prepare cocrystal solid dispersion: (1) to prepare cocrystal firstly and then mix it with polymer carrier to produce solid dispersion; (2) to melt the mixture of drug, coformer and polymer directly. Obviously, the second one is simple, solvent-free and low-cost. But this must be based on the premise that the mixture of drug and coformer can form cocrystal in polymer matrix during melting process. The previous work of other groups reported that the mixture of drug and coformer formed *in-situ* cocrystal during heating process (12) and the cocrystallization pathway was studied in details (13). Dhumal (14) also reported HME as a scalable, solvent-free, continous technology to prepare cocrystals in agglomerated form. Based on these reports, a hypothesis was proposed that drug and low T_m coformer probably *in-situ* cocrystallize in polymer carrier during heating process and then the mixture may melt at temperature much below the T_m of drug to produce amorphous solid dispersion without thermal degradation.

As a BCS class II drug with good permeability but poor water solubility, carbamazepine (CBZ) was widely studied to form cocrystal to improve dissolution behavior and decrease hygroscopicity (15,16). Most of the cocrystals showed much lower melting points than T_m of CBZ form I (190°C). As a heat-sensitive drug, there are many reports focused on its decomposition at high temperature (17,18).

In this paper, CBZ and nicotinamide (NIC) were selected as model drug and coformer, respectively, due to the lower melting point of their cocrystal (T_m=160°C). Amorphous CBZ-NIC cocrystal solid dispersions were prepared by melting method and HME at 160°C. The mechanism of *in-situ* cocrystallization in polymer carriers and the dissolution behaviors of solid dispersion were investigated. The aim of this study was to explore the formation of cocrystal as a novel approach to depress process temperature and minimize the thermal degradation of drug and polymer in preparing amorphous solid dispersion by MM and HME.

MATERIALS AND METHODS

Materials

Anhydrous CBZ was purchased from Yuancheng Technology Development Co., Ltd, Wuhan, China. Kollidon®VA64 (PVP/VA) and Soluplus® (SOLUPLUS) were friendly supplied by BASF Auxiliary Chemicals Co., Ltd., Shanghai, China. Hydroxypropyl methylcellulose E5 (2910 grade) (HPMC) was purchased from Colorcon Coating Technology Ltd., Shanghai, China. NIC was purchased form Aladdin Chemistry Co., Ltd., Shanghai, China. Methanol (HPLC grade) was purchased from Fischer Scientific, USA. All the reagents used were of analytical grade or better.

Thermal Gravimetric Analysis (TGA)

Thermal stability of the pharmaceutical components was evaluated by thermal gravimetric analysis (TGA) using NETZSCH STA-409 thermogravimetrical analyzer (NETZSCH group, Germany). Samples (5–10 mg) were heated in open aluminium pans to 300°C at a heating rate of 10°C/min. Nitrogen was used as purge gas at a flow rate of 30 ml/min. The data were analyzed using Proteus analysis software.

Differential Scanning Calorimetry (DSC)

Thermal behavior of the samples was examined by differential scanning calorimetry (DSC) (NETZSCH STA-409 thermogravimetrical analyzer, NETZSCH group, Germany). The accurately weighed samples (5–10 mg) were placed in open aluminiun pans and heated at 10°C/min to 210°C. Nitrogen at the flow rate of 30 ml/min was used as

purge gas, while the temperature ramp rate was 10°C/min. The instrument was calibrated using indium and the data were analyzed with Proteus analysis software.

Hot Stage Polarized Optical Microscopy (HSPM)

HSPM studies were conducted on a Leica DMPL polarizing optical microscope (Leica Microsystems Wetzlar Gmbh, Wetzlar, Germany). 5.00 mg CBZ and 2.58 mg NIC were weighed accurately at molar ratio of 1:1 for cocrystal formation experiment. The physical mixtures containing CBZ, NIC, and one of the three polymers (PVP/VA, SOLUPLUS and HPMC) also were weighed accurately at a weight ratio of 5.00: 2.58: 5.05. The blends were then mixed uniformly in a clean mortar. Each sample was placed between a glass slide and a cover glass and then fixed on Linkham THMS600 hot stage (Linkham Scientific Instruments Ltd., Surry, England). Then the sample was heated from ambient temperature to 200°C at 10°C/min. The morphology changes during the heating process were recorded by camera for further analysis.

Preparation of Cocrystal and Solid Dispersions by Melting Method (MM)

500 mg of CBZ and 258 mg of NIC (1:1 molar ratio) were mixed uniformly in a clean motar and then placed between two clean polyamide films, melted on a hot stage at 160°C for 5 min. The melt was cooled slowly at ambient condition for crystallization. The obtained CBZ-NIC cocrystal was pulverized in a mortar and passed through an 80-mesh sieve.

Similarly, a total weight of 500 mg of CBZ and PVP/VA (40:60 w/w), and CBZ, NIC and PVP/VA (40:20:40 w/w) were mixed, melted and cooled at same conditions as above to form solid dispersions. The obtained CBZ-PVP/VA and CBZ-NIC-PVP/VA solid dispersions were pulverized and passed through an 80-mesh sieve. The final powders were kept in a desiccator for further analysis. Examination by X-ray powder diffraction did not show any change in physical state of solid dispersion after grinding.

Hot Melt Extrusion (HME)

Hot melt extrusion was conducted using a conical co-rotating (5–14 mm diameter) twin screw HAAKE MiniLab II Microcompounder (Thermo Electron GmbH, Karlsruhe). The extrusion temperature and screw speed were fixed at 160°C and 30 rpm, respectively.

According to the formulations given in Table 1, the materials were accurately weighed, premixed in a clean mortar, and then manually fed into the extruder. The residence time of the materials in the extruder was about 1 min. Part of the melt extrudates were pressed into round slices immediately for X-ray powder diffraction characterization; the others were cooled at ambient condition, milled with an impact mill and then passed through an 80-mesh sieve to yield a final powder for further analysis.

X-ray Powder Diffraction (XRPD)

X-ray diffractometer with Cu Kα radiation (Rigaku D/Max 2000, Japan) was used to determine the crystallinity of samples at ambient temperature. The generator voltage and current were 40 kV and 30 mA, respectively. The 2-theta scanning range was from 3 to 40° at a rate of 5°/min and a step size of 0.02°. Verification of the instrument was performed using mica and alumina reference standards.

Optical Microscopy

Morphology of the solid dispersions was observed using an Olympus optical microscope (IX71, Olympus Corporation, Japan) with a magnification range of 4×.

Fourier Transform Infrared Spectroscopy (FTIR)

Intermolecular hydrogen bonding between drug and excipients was determined using Fourier transform infrared spectrometer equipped with a KBr beam splitter (TENSOR37, Bruker, Germany). Sample powders were mixed with dry KBr (IR, spectroscopy grade, China) in a ratio of 1:100 and compressed into semitransparent pellets by applying a pressure of 10 tonnes for 1 min. The scan range was 400–4,000 cm^{-1}, using 64 scans per spectrum with a resolution of 4 cm^{-1}. Samples were examined in the transmission mode and software Bruker OPUS 6.5 was used for data analysis.

In Vitro Dissolution Study

Dissolution behaviors of the micronized solid dispersions were studied using a USP paddle dissolution apparatus (ZRS-8 G dissolution tester, Tianda Tianfa Technology Co., Ltd., China). All release studies were carried out at a temperature of 37 ± 0.5°C and a stirring rate of 100 rpm in 900 ml of distilled water. Samples equivalent to 20 mg of CBZ were accurately weighed and added to the dissolution medium. At time points of 5, 10, 20, 30, 60, 75, 90 and 120 min, 5 ml of aliquots were taken and immediately replaced with an equal volume of fresh dissolution medium. The aliquot samples were filtered with a 0.45 μm filter. The first 2 ml of filtrate was discarded and the remainder was analyzed by high-performance liquid chromatography (HPLC). Each study was performed in triplicate.

Table I Formulation of Solid Dispersions

Formulation	Components (% w/w)					Manufacturing technique
	CBZ	NIC	PVP/VA	SOLUPLUS	HPMC	
CBZ-PVP/VA	40	–	60	–	–	MM and HME
CBZ-NIC-PVP/VA	40	20	40	–	–	MM and HME
CBZ-SOLUPLUS	40	–	–	60	–	HME
CBZ-NIC-SOLUPLUS	40	20	–	40	–	HME
CBZ-HPMC	40	–	–	–	60	HME
CBZ-NIC-HPMC	40	20	–	–	40	HME

High Performance Liquid Chromatography (HPLC)

Concentration of CBZ in samples was determined by a Shimadzu LC-20AT HPLC system (Shimadzu Corporation, Japan) at the wave length of 285 nm using a Waters Xbridge Shied RP-18, 5 μm×4.6 mm×250 mm column (Waters Corporation, USA). All measurements were performed with the injection volume of 20 μL, a mixture of methanol (70%) and water (30%) as the mobile phase pumped at a flow rate of 0.9 ml/min, and at temperature of 40°C using a column oven. These conditions resulted in a typical elution time of 4.7 min for CBZ. Calibration curves were constructed using standard solutions of known concentration and Shimadzu software was used to calculate the peak area automatically.

RESULTS

Thermal Stability of CBZ

Chemical stability of all components at elevated temperature is an essential prerequisite for a successful solid dispersion production prepared by MM and HME. PVP/VA and NIC were reported to be thermally stable at the processing temperature of MM and HME (19,20). The thermal stability of CBZ was investigated using TGA and the results were shown in Fig. 1. The thermogravimetric profiles showed that CBZ was stable up to 160°C. When the temperature increased to the melting point of CBZ form I (T_m=190°C), the weight loss was 1.35%. As the temperature over 190°C, CBZ started to decompose seriously and the weight loss increased dramatically. The results imply that it is difficult to prepare chemically stable amorphous solid dispersion of CBZ by MM and HME because heating above the T_m of drug to convert crystalline into amorphous will lead to significant degradation of CBZ. Therefore, it is necessary to decrease the T_m of CBZ in order to prepare amorphous solid dispersion at lower temperature and avoid the thermal degradation.

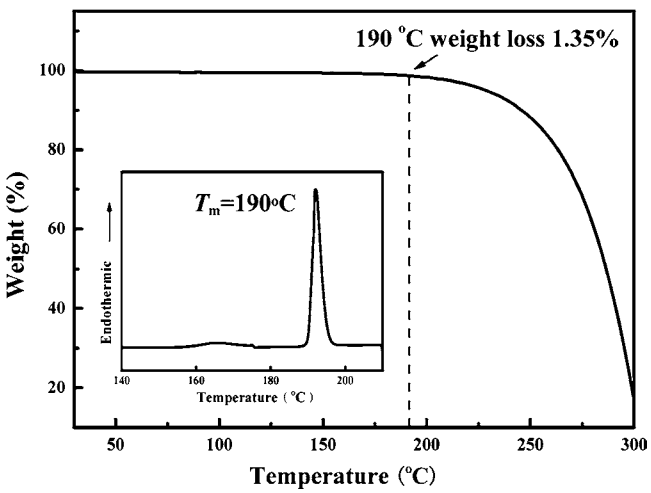

Fig. 1 Thermogravimetric and DSC thermograms of CBZ.

DSC Analysis

The thermal behavior and crystalline phase transformation of CBZ, NIC, CBZ-NIC cocrystal and physical mixture during the melting processing were investigated by DSC and the thermograms were shown in Fig. 2. CBZ exhibited enantiotropic polymorphism and showed a small melting endotherm at 160°C followed by a second endotherm at 190°C. These two endotherms were attributed to the melting of original form III and melt-recrystallized form I of CBZ, respectively (21). Pure NIC and CBZ-NIC cocrystal prepared by melting method showed a single melting peak around 130°C and 160°C, respectively, in agreement with the previous reports (20,22).

For CBZ-NIC physical mixture, the DSC trace showed two sharp endothermic peaks and one small exothermic peak around 140°C. The first peak reflected the melting of NIC at 130°C. Then CBZ crystalline dissolved in the molten NIC followed by an immediate exothermic cocrystallizaiton process, which generated a small crystallization peak around 140°C. The formed cocrystal showed a melting peak around 160°C.

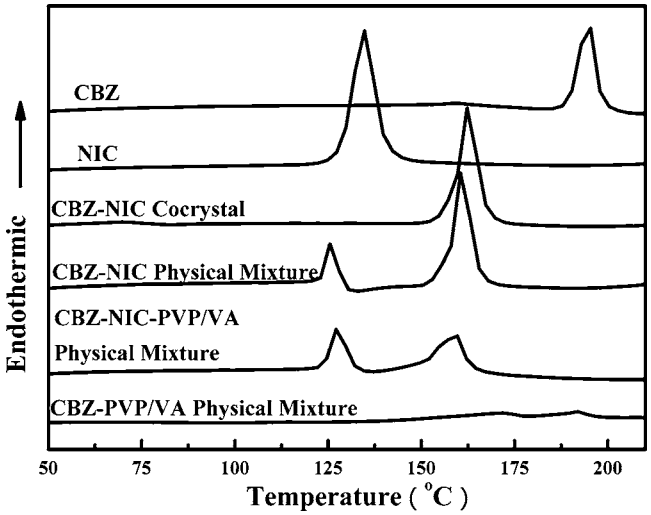

Fig. 2 DSC thermograms of CBZ, NIC, CBZ-NIC cocrystal and the physical mixtures.

CBZ-NIC-PVP/VA physical mixture showed a similar behavior as CBZ-NIC physical mixture which indicated the *in-situ* formation of CBZ-NIC cocrystal in PVP/VA. The DSC curve of CBZ-PVP/VA physical mixture showed two endothermic peaks around 170°C and 190°C corresponding to the transformation of CBZ from form III to form I.

The DSC results suggested CBZ and NIC could *in-situ* cocrystallize in PVP/VA during heating process and the cocrystal would melt at about 160°C.

HSPM Investigation

The crystallization pathways of CBZ and NIC in polymer carriers were further investigated with HSPM and the photomicrographs collected were shown in Fig. 3. For CBZ, the agglomerates of prismatic crystal corresponding to form III (23) converted to small needle-like crystal corresponding to form I (24) from 173°C and finally form I crystal melted at 191°C (shown in Fig. 3a). For NIC, the crystalline completely melted at 135°C. For CBZ-NIC physical mixture, NIC melted from 130°C and CBZ dissoluted into NIC melt (the microphotograph was not presented here). Then, CBZ-NIC cocrystal began to grow until 157°C and completely melted at 164°C (shown in Fig. 3b). The similar phenomena were observed in physical mixtures of CBZ-NIC-PVP/VA and CBZ-NIC-SOLUPLUS (shown in Fig. 3c). The polymer matrix didn't disturb the formation and melting of CBZ-NIC cocrystal. However, in CBZ-NIC-HPMC system, part of crystal melted around 165°C and part of them remained until 190°C (shown in Fig. 3c).

The results of DSC and HSPM analysis indicated that CBZ and NIC could *in-situ* form cocrystal in polymer matrix during heating process. The newly generated cocrystal might melt at 160°C and be completely dispersed in polymer carrier to form amorphous solid dispersion if the cooling process is controlled properly. Based on these performulation studies, it can be proposed that the mixture of CBZ, NIC and polymer carrier may be melted directly to prepare amorphous cocrystal solid dispersion by MM or HME at 160°C, which is 30°C below the melt point of CBZ form I. The exceptional system with HPMC as carrier was discussed specially in the discussion section.

Characterization of Solid Dispersions Prepared by Melting Method

XRPD Characterization

The solid state of all raw materials, CBZ-PVP/VA and CBZ-NIC-PVP/VA solid dispersions, and the corresponding physical mixtures was studied by XRPD as shown in Fig. 4 a-b. PVP/VA was amorphous, and NIC showed the characteristic diffraction peaks at $2\theta = 14.9°$, while CBZ showed the characteristic peaks at $2\theta = 15.4$, 19.6, 25.0 and 27.5°, corresponding to form III (25). CBZ-NIC cocrystal prepared by melting method exhibited characteristic peaks at $2\theta = 6.9$, 10.4, 18.1, 20.6 and 26.6° and this was in agreement with previous report (26). The characteristic peaks of CBZ and NIC were strong in all of the physical mixtures, which implied that simply mixing couldn't change the physical state of each component. No diffraction peaks were observed in the pattern of CBZ-NIC-PVP/VA solid dispersion which indicated CBZ-NIC cocrystal was in an amorphous or molecular state in the solid dispersion. However, diffraction peaks of CBZ-PVP/VA solid dispersion reflected a small amount of CBZ crystalline remained in the dispersion and this could be attributed to the incomplete fusion of CBZ in PVP/VA at 160°C below its T_m.

FTIR Characterization

Possible interactions between the components in solid dispersion were investigated by FTIR, as shown in Fig. 5. The spectrum of pure CBZ showed peaks at 3,465 and 3,157 cm^{-1} corresponding to free anti-NH and hydrogen bonded syn-NH respectively. Peaks corresponding to NH_2 and carbonyl stretch of the amide were also observed in the spectrum of NIC, and peaks at 3,367 and 3,163 cm^{-1} might be attributed to the anti-symmetric and symmetric stretching vibrations of NH_2 group, respectively. The FTIR spectrum of CBZ-NIC physical mixture showed most of the characteristic peaks of CBZ and NIC. CBZ was previously reported to form cocrystal with NIC via crystallization from melting (13), co-milling (26) and solution (22) and the crystal structure of CBZ-NIC cocrystal is characterized by

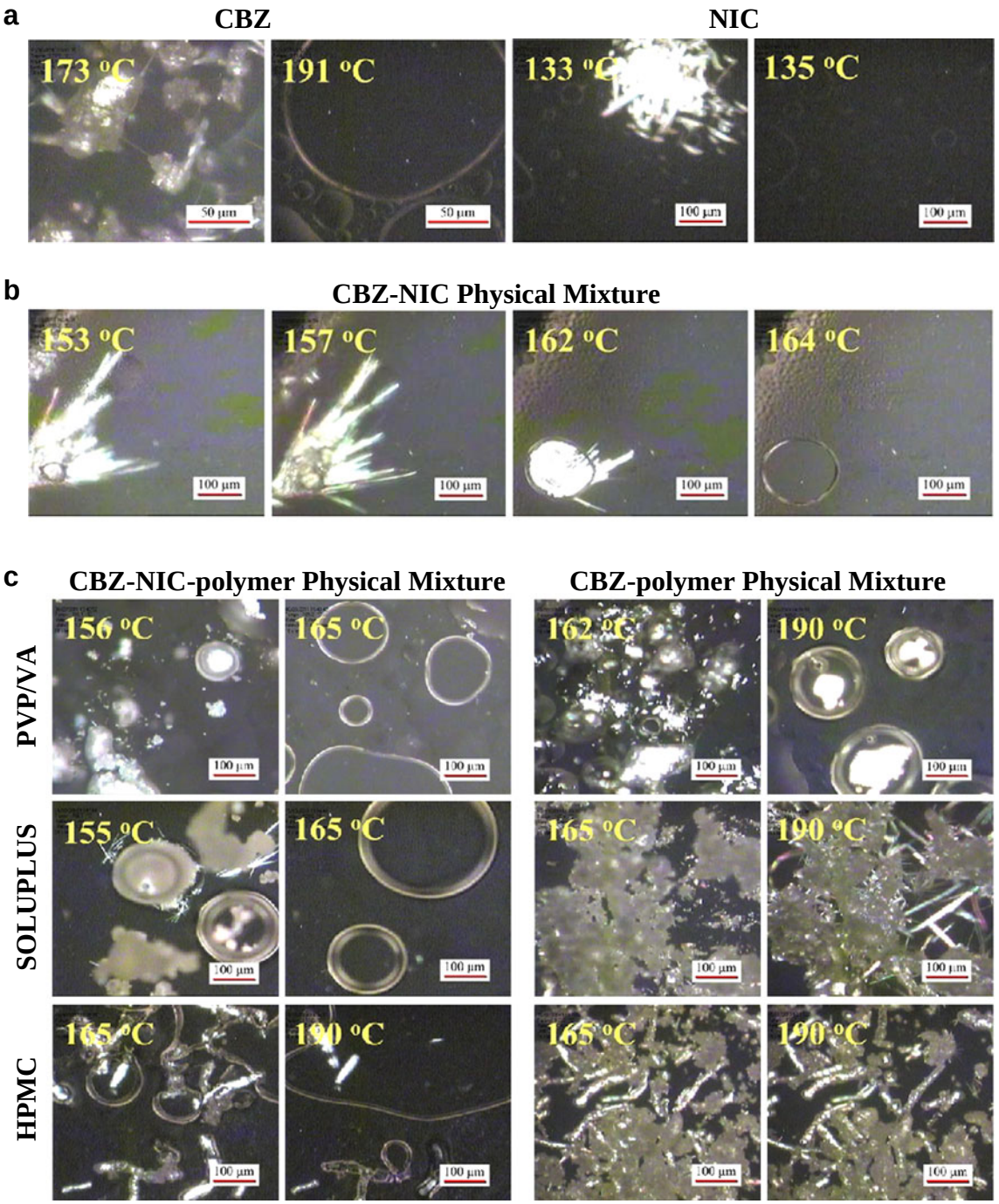

Fig. 3 HSPM micrographs of phase transition during heating processes: (**a**) CBZ and NIC; (**b**) CBZ-NIC physical mixture; (**c**) CBZ-NIC-polymer and CBZ-polymer physical mixtures.

NH···O=C hydrogen bonds between CBZ and NIC (27). The shift of NH_2 peak of NIC from 3,367 cm^{-1} to 3,389 cm^{-1} suggested the interactions existed between CBZ and NIC during co-milling (26). As shown in Fig. 5, peak shifts corresponding to NH stretch of the amide were observed from 3,465 to 3,157 cm^{-1} for CBZ to 3,447 and 3,389 cm^{-1} for the cocrystal, respectively. This may be attributed to the hydrogen bonding between CBZ and NIC which facilitates the formation of CBZ-NIC cocrystal. Similar spectral patterns were observed in indomethacin-NIC melt (28) and ibuprofen-NIC complex (29).

The FTIR spectra of CBZ-NIC-PVP/VA and CBZ-PVP/VA physical mixtures seemed to be a simple summation of drug and excipient spectra, indicating that there were little

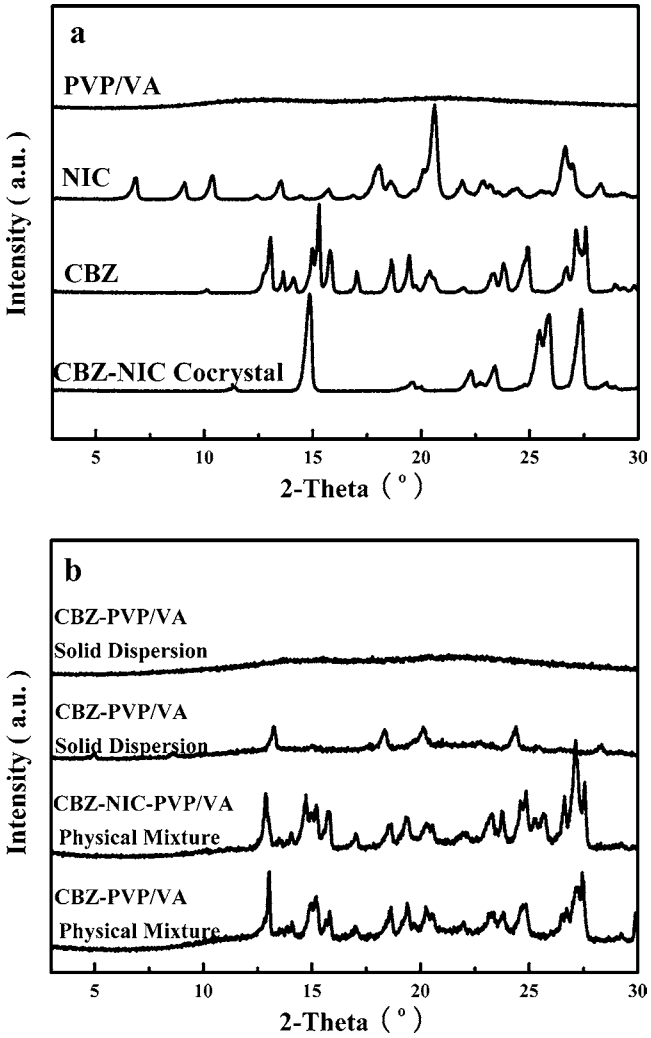

Fig. 4 XRPD patterns of pure components (**a**) and solid dispersions prepared by MM and corresponding physical mixtures (**b**).

interactions between CBZ, NIC and PVP/VA in physical mixture. However, substantial differences were observed in spectrum of CBZ-NIC-PVP/VA solid dispersion. Two peaks at 3,465 and 3,157 cm^{-1} for N-H stretching vibrations of primary amide groups of CBZ were replaced by a broader peak at 3,447 cm^{-1} in spectrum of solid dispersion. This indicated the possible involvement of $-NH_2$ group in hydrogen bonding with C=O group of NIC. On the other hand, the spectrum of CBZ-PVP/VA solid dispersion displayed a distinctive peak at 3,465 cm^{-1} and a less intensive peak at 3,157 cm^{-1}, which may be related to residual CBZ crystalline in CBZ-PVP/VA solid dispersion and this is consistent with DSC, XRPD and HSPM results.

Dissolution Studies

Dissolution behavior of pure CBZ, CBZ-NIC cocrystal, solid dispersions and the corresponding physical mixtures were studied and the dissolution profiles were shown in Fig. 6. The results were given as percentage dissolved as a proportion of the total amount of drug in each sample. Due to the poor wettability and agglomeration, the dissolution of pure CBZ was poor and maximumly about 60% of the drug was released after 120 min. The dissolution rate of CBZ-NIC cocrystal was faster than that of CBZ. The two physical mixtures showed slight improvement in dissolution rate compared to pure CBZ due to the hydrophilic properties of NIC and PVP/VA which might act as solubilizing agents for CBZ. The same result can be found in the formulation containing CBZ-NIC cocrystal and cyclodextrin (30). For CBZ-PVP/VA solid dispersion, about 67% of CBZ was released within 20 min which clearly demonstrated the improvement of CBZ through solid dispersion technique. With the addition of NIC, CBZ-NIC-PVP/VA solid dispersion exhibited more rapid dissolution and approximately 100% of CBZ was released within 20 min.

Characterization of Solid Dispersion Prepared by Hot Melt Extrusion

XRPD and Optical Microscopy Analysis

The physical state of solid dispersions prepared by HME was characterized by XRPD and the diffractograms were shown in Fig. 7. The diffraction profiles of CBZ-polymer solid dispersions showed small diffraction peaks, indicating the presence of crystalline CBZ residue in the products. The peak intensity of CBZ in SOLUPLUS was weaker than that in PVP/VA and HPMC. This phenomenon may be attributed to the lower T_g of SOLUPLUS (70°C) (31)

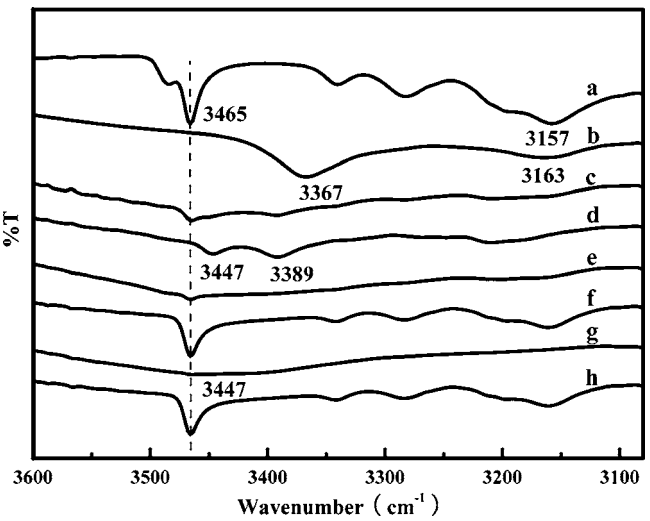

Fig. 5 FTIR spectra of CBZ (**a**), NIC (**b**), CBZ-NIC physical mixture (**c**), CBZ-NIC cocrystal (**d**), CBZ-PVP/VA solid dispersion (**e**), CBZ-PVP/VA physical mixture (**f**), CBZ-NIC-PVP/VA solid dispersion (**g**) and CBZ-NIC-PVP/VA physical mixture (**h**).

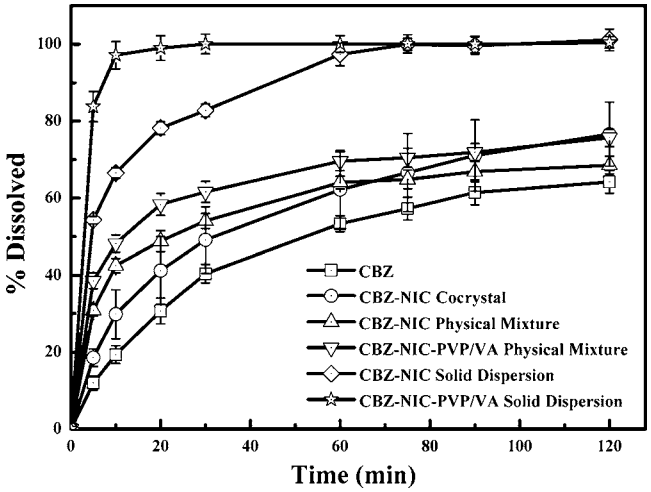

Fig. 6 Dissolution profiles of CBZ, CBZ-NIC cocrystal, solid dispersions prepared by MM and the corresponding physical mixtures ($n = 3$).

compared with PVP/VA (102°C) (32) and HPMC (165°C) (33). Part of crystalline CBZ dissolved in the molten polymer with a forced convective diffusion process. However, the processing temperature below the T_m of CBZ couldn't ensure complete conversion of CBZ from crystalline to amorphous form during HME. With incorporation of NIC, few diffraction peaks were displayed suggesting the amorphous state of the products.

The morphologies of the solid dispersion were observed by optical microscopy and the results were shown in Fig. 8. Consistently, considerable amount of undissolved drug particulates were observed in CBZ-polymer solid dispersion. For CBZ-NIC-polymer solid dispersion, no drug crystalline was observed which indicated NIC and CBZ were completely converted into amorphous state. The spots with regular shape and dark edge observed in CBZ-NIC-PVP/VA solid dispersion were air bubbles trapped in the polymer carrier.

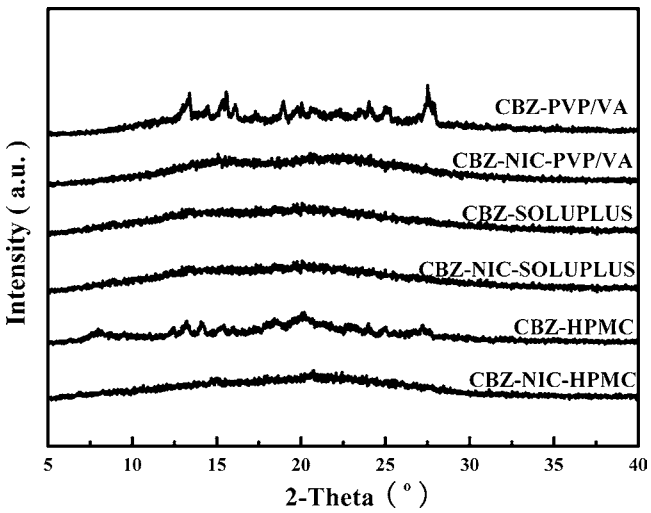

Fig. 7 XRPD patterns of solid dispersions prepared by HME.

Dissolution Studies

Figure 9a–c showed the dissolution profiles of solid dispersions prepared by HME with different polymer carriers and the corresponding physical mixtures. Overall, the drug in physical mixtures dissolved slowly and maximumly less than 80% of CBZ was released over 120 min, while CBZ in CBZ-polymer extrudates dissolved completely to 100% in 60 min. With the incorporation of NIC, the complete dissolution of drug was accelerated from 60 min to 20 min for all three CBZ-NIC-polymer solid dispersions. These results demonstrated the remarkable effect of NIC on the enhancement of CBZ dissolution from solid dispersions through improving the dispersibility of solid dispersion and the solubilizing effect.

DISCUSSION

The main aim of this study was to prove cocrystallization as an effective approach to avoid thermal degradation of heat-sensitive drug during HME and MM. Firstly, it was proved that CBZ-NIC cocrystal at molar ratio of 1:1 could be *in-situ* formed in three polymer carriers during heating process based on DSC and HPSM characterization. And the newly formed cocrystal completely melted around 160°C, which is 30°C lower than the T_m of CBZ. This means amorphous CBZ-NIC-polymer solid dispersion may be prepared at processing temperature significantly lower than T_m of CBZ by simply adding NIC into CBZ-polymer physical mixture. Secondly, two methods, MM and HME, were used to prepare solid dispersions and prove this speculation. The difference between the two methods is the additional shear force during HME. Amorphous CBZ-NIC-polymer solid dispersions were successfully prepared at 160°C using both MM and HME, and showed improved dissolution behavior than CBZ-polymer solid dispersions.

The Miscibility and Melting Point Depression of Three Polymers

Solubility parameter (δ) calculated by Van Krevelen method and Fedors method was introduced to understand the miscibility between CBZ and the polymers. The average δ values calculated by two methods for CBZ, PVP/VA, SOLUPLUS and HPMC were 23.9, 22.8, 18.4 and 26.4 $MPa^{1/2}$, respectively. The differences of δ values between CBZ and polymers were ranging from 1.1 to 5.4 indicating good miscibility between CBZ and polymers (34).

For miscible drug-polymer systems, depression of melting point of drug was a well documented phenomenon (35–38). The depression extent is affected by many factors, such

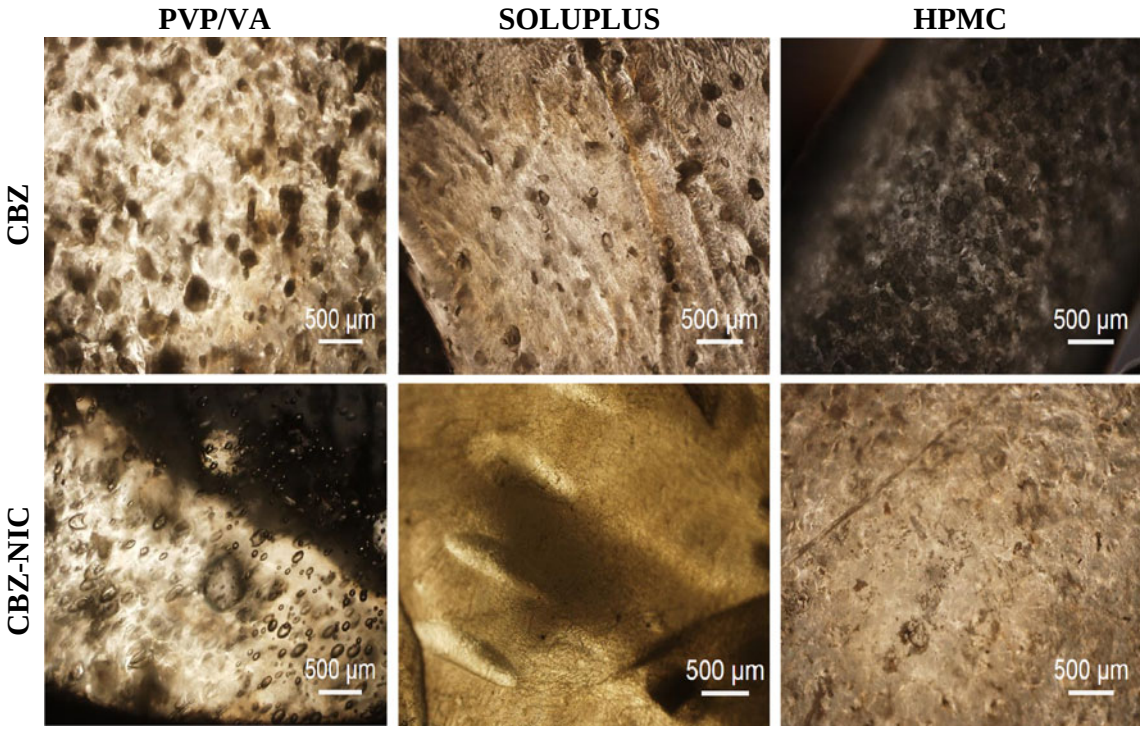

Fig. 8 Photomicrographs of solid dispersions prepared by HME.

as drug loading, T_g of polymer, heating rate, and the particle size of both drug and polymer. If T_g of polymer is higher than T_m of drug, no depression phenomenon can be observed (37). The higher drug loading resulted in weaker depression effect (36,37). In the present study, 40% drug loading was relatively high. Therefore, no distinct depression of melting point was observed for CBZ-polymer systems in DSC (Fig. 2) and HSPM experiments (Fig. 3), and some CBZ crystalline still remained at 190°C.

Possible Interactions Between NIC and HPMC

For CBZ-NIC-PVP/VA and CBZ-NIC- SOLUPLUS systems, all of the crystalline melted around 160°C as expected. However, for CBZ-NIC-HPMC system, HSPM microphotograms showed that even at 165°C (above T_m of CBZ-NIC cocrystal, 160°C), some crystalline still remained in the melt and complete fusion was observed at 190°C. This exceptional phenomenon may be attributed to the competition between HPMC and CBZ to form hydrogen bonds with NIC. Based on previous reports, HPMC dissolved in NIC melt at 140°C and formed intermolecular hydrogen bonds with NIC molecules (39). In current experiment, both CBZ and HPMC had the tendency to interact with NIC through hydrogen bonds. If HPMC occupied part of hydrogen bonding sites of NIC, there were no enough sites left for CBZ to form CBZ-NIC cocrystal because CBZ and NIC were blended at molar ratio of 1:1 and the stoichiometry of CBZ-NIC cocrystal was also 1:1. The unbounded CBZ crystals didn't melt at 160°C and remained in CBZ-NIC-HPMC solid dispersion. However, the amount of residual crystalline is very small because XRD patterns didn't exhibit distinct crystal diffraction peaks within the limit of detection. Also the trace of crystalline in CBZ-NIC-HPMC did not slow down the dissolution of CBZ as shown in Fig. 9c. Certainly, the competition mechanism between CBZ and HPMC needs further study.

Comparison of Dissolution Behavior and Hydrotropism of NIC

To further confirm the cocrystallization method can be applied for different polymer systems rather than a special case and to optimize the CBZ-NIC-polymer formulations, three water soluble polymers, PVP/VA, SOLUPLUS and HPMC, were selected for HME experiment based on the miscibility and the extrusion temperature range.

For CBZ-polymer solid dispersion, CBZ-SOLUPLUS showed more rapid dissolution rate than the other two systems. It may be attributed to the amphiphilic structure of SOLUPLUS which can solubilize water insoluble drug through micelle formation in water (31,40). However, the dissolution profiles of CBZ-NIC-polymer extrudates prepared by HME were less polymer dependent. For all three solid dispersions, CBZ released 100% within 20 min and

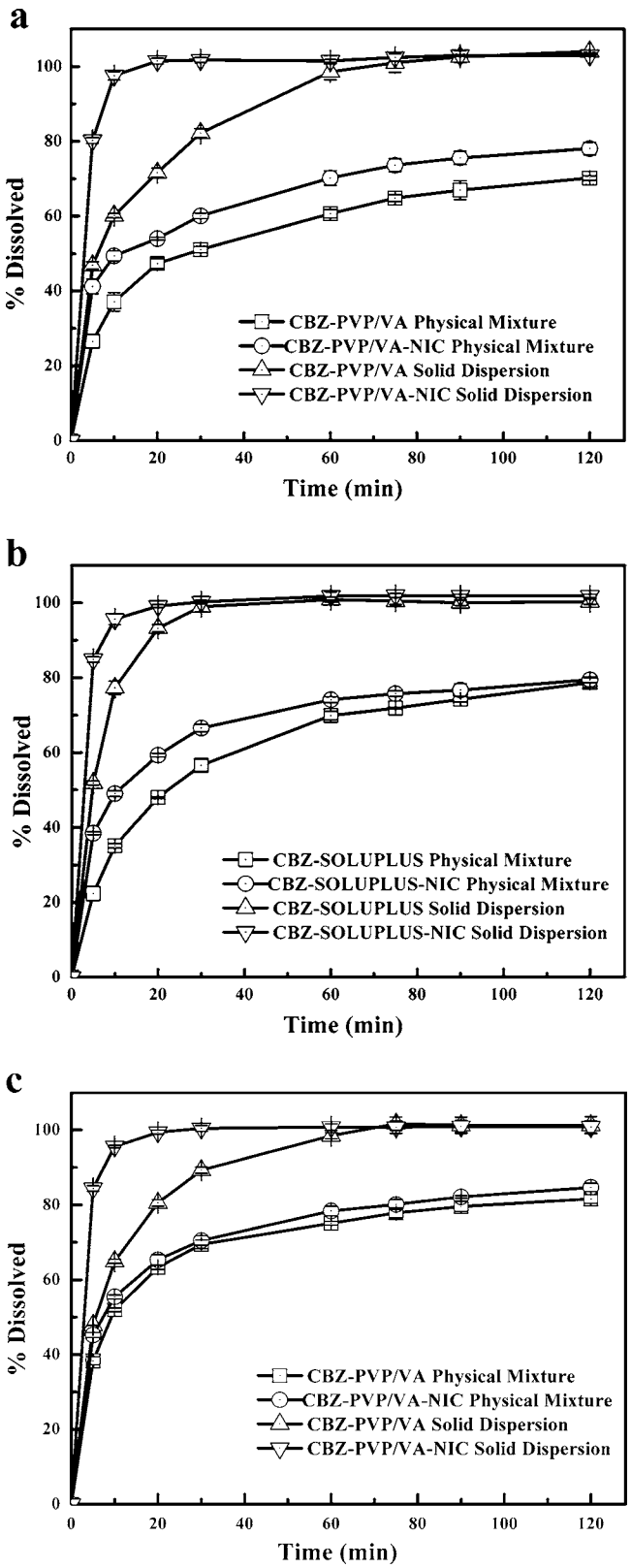

Fig. 9 Dissolution profiles of solid dispersions prepared by HME and corresponding physical mixtures with different polymer carriers: (**a**) PVP/VA; (**b**) SOLUPLUS; (**c**) HPMC ($n = 3$).

there was no remarkable difference in dissolution behavior between each other. This phenomenon is very likely due to the solubilizing effect of NIC and the water soluble polymer matrix, together with the good dispersion and amorphous state of CBZ.

Compared with CBZ-polymer solid dispersion, CBZ-NIC-polymer solid dispersion exhibited faster dissolution rate. Two factors probably accounted for this phenomenon: (1) *in-situ* formed CBZ-NIC cocrystal melted and dispersed as amorphous or molecular state in polymer matrix. That means, CBZ is completely in amorphous state in CBZ-NIC-polymer solid dispersion but partly in crystalline state in CBZ-polymer solid dispersion. It is well known amorphous drug generally dissolves faster than the relevant crystalline form because there is no lattice energy to be overcome. (2) NIC was reported as a hydrotropic agent to solubilize a wide variety of drugs through forming complex with drugs (41–45) or changing the nature of solvent, especially by altering the solventing ability via intermolecular hydrogen bonding (46). Here, NIC probably acted as a solubility enhancer to help CBZ dissolve faster through hydrogen bonding. However, this hydrotropic solubilization mechanism for CBZ-NIC system needs further research. At the same time, all of the three polymers are water soluble and they also promoted the solubility of CBZ. The synergistic solubilizing effects of both polymer and NIC made CBZ release 100% within 20 min from CBZ-NIC-polymer solid dispersion. In comparison, single solubilizing effect of polymer in CBZ-polymer solid dispersion resulted in slower release of CBZ.

CONCLUSIONS

In current study, *in-situ* formation of cocrystal was proved to be an effective approach to prepare chemically stable solid dispersions for heat-sensitive and poorly water-soluble drugs. Amorphous CBZ-NIC-polymer solid dispersions were successfully prepared by both MM and HME at processing temperature significantly below the melting point of drug. Furthermore, CBZ released completely from the solid dispersions within 20 min, and the dissolution improvement was little polymer matrix dependent. The extrusion temperature range can also be adjusted by selecting different coformer. However, the effect of coformer on the properties of drug must be considered, such as recrystallization tendency, physical stability, hygroscopicity, pharmacokinetics, and pharmacology.

ACKNOWLEDGMENTS & DISCLOSURES

This work was supported by Guangdong Research Center for Drug Delivery Systems (No. GCZX-A0801). We are grateful

to Mrs. Aiping Huang for the help of HSPM experiment. We are also acknowledging Thermo Fisher Scientific (China) Co., Ltd. for the help of HME experiment.

REFERENCES

1. Vasconcelos T, Sarmento B, Costa P. Solid dispersions as strategy to improve oral bioavailability of poor water soluble drugs. Drug Discov Today. 2007;12(23–34):1068–75.
2. Chokshi RJ, Zia H, Sandhu HK, Shah NH, Malick WA. Improving the dissolution rate of poorly water soluble drug by solid dispersion and solid solution: pros and cons. Drug Deliv. 2007;14(1):33–45.
3. Lalkshman JP, Cao Y, Kowalski J, Serajuddin ATM. Application of melt extrusion in the development of a physically and chemically stable high-energy amorphous solid dispersion of a poorly water-soluble drug. Mol Pharm. 2008;5 (6):994–1002.
4. Liu HJ, Wang P, Zhang XY, Shen F, Gogos CG. Effects of extrusion process parameters on the dissolution behavior of indomethacin in Eudragit (R) E PO solid dispersions. Int J Pharm. 2010;383(1–2):161–9.
5. Repka MA, Battu SK, Upadhye SB, Thumma S, Crowley MM, Zhang F, *et al.* Pharmaceutical applications of hot-melt extrusion: Part II. Drug Dev Ind Pharm. 2007;33(10):1043–57.
6. Crowley MM, Zhang F, Repka MA, Thumma S, Upadhye SB, Battu SK, *et al.* Pharmaceutical applications of hot-melt extrusion: Part I. Drug Dev Ind Pharm. 2007;33(9):909–26.
7. Munjal M, Stodghill SP, Elsohly MA, Repka MA. Polymeric systems for amorphous Delta(9)-tetrahydrocannabinol produced by a hot-melt method. Part 1: chemical and thermal stability during processing. J Pharm Sci. 2006;95(8):1841–53.
8. Verreck G, Decorte A, Heymans K, Adriaensen J, Liu D, Tomasko D, *et al.* Hot stage extrusion of p-amino salicylic acid with EC using CO_2 as a temporary plasticizer. Int J Pharm. 2006;327(1–2):45–50.
9. Wu CB, McGinity JW. Influence of methylparaben as a solid-state plasticizer on the physicochemical properties of Eudragit (R) RS PO hot-melt extrudates. Eur J Pharm Biopharm. 2003;56(1): 95–100.
10. Ghebremeskel AN, Vernavarapu C, Lodaya M. Use of surfactants as plasticizers in preparing solid dispersions of poorly soluble DRUG: Selection of polymer-surfactant combinations using solubility parameters and testing the processability. Int J Pharm. 2007;328(2):119–29.
11. Schultheiss N, Newman A. Pharmaceutical cocrystals and their physicochemical Properties. Cryst Growth Des. 2009;9(6):2950–67.
12. Lu E, Rodriguez-Hornedo N, Suryanarayanan R. A rdrugd thermal method for cocrystal screening. Cryst Eng Comm. 2008;10(6): 665–8.
13. Seefeldt K, Miller J, Alvarez-Nunez F, Rodríguez-Hornedo N. Crystallization pathways and kinetics of carbamazepine-nicotinamide cocrystals from the amorphous state by *in situ* thermomicroscopy, spectroscopy, and calorimetry studies. J Pharm Sci. 2007;96(5):1147–58.
14. Dhumal RS, Kelly AL, York P, Coates PD, Paradkar A. Cocrystalization and simultaneous agglomeration using hot melt extrusion. Pharm Res. 2010;27(12):2725–33.
15. Childs SL, Wood PA, Rodríguez-Hornedo N, Reddy LS, Hardcastle KI. Analysis of 50 crystal structures containing carbamazepine using the materials module of mercury CSD. Cryst Growth Des. 2009;9(4):1869–88.
16. Good DJ, Rodríguez-Hornedo N. Solubility advantage of pharmaceutical cocrystals. Cryst Growth Des. 2009;9(5):2252–64.
17. Griesser U, Szelagiewicz M, Hofmeier U, Pitt C, Cianferani S. Vapor pressure and heat of sublimation of crystal polymorphs. J Therm Anal Calorim. 1999;57(1):45–60.
18. Krahnand FU, Mielck JB. Effect of type and extent of crystalline order on chemical and physical stability of carbamazepine. Int J Pharm. 1989;53(1):25–34.
19. DiNunzio JC, Brough C, Hughey JR, Miller DA, Williams RO, McGinity JW. Fusion production of solid dispersions containing a heat-sensitive active ingredient by hot melt extrusion and Kinetisol (R) dispersing. Eur J Pharm Biopharm. 2010;74 (2):340–51.
20. Moreschi ECP, Matos JR, Almeida-Muradian LB. Thermal analysis of vitamin PP Niacin and niacinamide. J Therm Anal Calorim. 2009;98(1):161–4.
21. Grzesiak AL, Lang M, Kim K, Matzger AJ. Comparison of the four anhydrous polymorphs of carbamazepine and the crystal structure of form I. J Pharm Sci. 2003;92(11):2260–71.
22. Fleischman SG, Kuduva SS, McMahon JA, Moulton B, Bailey Walsh RD, Rodríguez-Hornedo N, *et al.* Crystal engineering of the composition of pharmaceutical phases: multiple-component crystalline solids involving carbamazepine. Cryst Growth Des. 2003;3(6):909–19.
23. Katzhendler I, Azoury R, Friedman M. Crystalline properties of carbamazepine in sustained release hydrophilic matrix tablets based on hydroxypropyl methylcellulose. J Control Release. 1998;54(1):69–85.
24. Rustichelli C, Gamberini G, Ferioli V, Gamberini MC, Ficarra R, Tommasini S. Solid-state study of polymorphic drugs: carbamazepine. J Pharmaceut Biomed. 2000;23(1):41–54.
25. Harris RK, Ghi PY, Puschmann H, Apperley DC, Griesser UJ, Hammond RB, *et al.* Structural studies of the polymorphs of carbamazepine, its dihydrate, and two solvates. Org Process Res Dev. 2005;9(6):902–10.
26. Chieng N, Hubert M, Saville D, Rades T, Aaltonen J. Formation kinetics and stability of carbamazepine-nicotinamide cocrystals prepared by mechanical activation. Cryst Growth Des. 2009;9 (5):2377–86.
27. Rodríguez-Hornedo N, Nehm SJ, Seefeldt KF, Pagán-Torres Y, Falkiewicz CJ. Reaction crystallization of pharmaceutical molecular complexes. Mol Pharm. 2006;3(3):362–7.
28. Bogdanova S, Sidzhakova D, Karaivanova V, Georgieva S. Aspects of the interactions between indomethacin and nicotinamide in solid dispersions. Int J Pharm. 1998;163(1–2):1–10.
29. Oberoi LM, Alexander KS, Riga AT. Study of interaction between ibuprofen and nicotinamide using differential scanning calorimetry, spectroscopy, and microscopy and formulation of a fast-acting and possibly better ibuprofen suspension for osteoarthritis patients. J Pharm Sci. 2005;94(1):93–101.
30. Shikhar A, Bommana MM, Gupta SS, Squillante E. Formulation development of Carbamazepine-Nicotinamide co-crystals complexed with γ-cyclodextrin using supercritical fluid process. J Supercrit Fluids. 2011;55(3):1070–8.
31. Hardung H, Djuric D, Ali S. Combining HME & solubilization: Soluplus®- The solid solution. Drug Delivery Tech. 2010;10 (3):20–7.
32. Matsumoto T, Zografi G. Physical Properties of solid molecular dispersions of indomethacin with poly(vinylpyrrolidone) and poly (vinylpyrrolidone-co-vinyl-acetate) in relation to indomethacin crystallization. Pharm Res. 1999;16(11):1722–8.
33. McPhillips H, Craig DQM, Royall PG, Hill VL. Characterisation of the glass transition of HPMC using modulated temperature differential scanning calorimetry. Int J Pharm. 1999;180(1):83–90.

34. Greenhalgh DJ, Williams AC, Timmins PT, York P. Solubility parameters as predictors of miscibility in solid dispersions. J Pharm Sci. 1999;88(11):1182–90.
35. Broman E, Khoo C, Taylor LS. A comparison of alternative polymer excipients and processing methods for making solid dispersions of a poorly water soluble drug. Int J Pharm. 2001;222 (1):139–51.
36. Bartsch SE, Griesser UJ. Physicochemical properties of the binary system glibenclamide and polyethylene glycol 4000. J Therm Anal Calorim. 2004;77(2):555–69.
37. Marsac PJ, Shamblin SL, Taylor LS. Theoretical and practical approaches for prediction of drug-polymer miscibility and solubility. Pharm Res. 2006;23(10):2417–26.
38. Marsac PJ, Li TL, Taylor LS. Estimation of drug–polymer miscibility and solubility in amorphous solid dispersions using experimentally determined interaction parameters. Pharm Res. 2009;26(1):139–51.
39. Hino T, Ford JL. Characterization of the hydroxypropylmethylcellulose—nicotinamide binary system. Int J Pharm. 2001;219(1–2):39–49.
40. Djuric D, Boyko V, Karl M and Kolter K. Characterization of polymeric micelles from solid solutions with a polyvinyl caprolactam-polyvinyl acetate-polyethylene glycol graft copolymer and itraconazole. CRS 2011 38th Annual Meeting & Exposition of the Gontrolled Release Society, July 30–August 3, 2011, National Harbor, Maryland, USA.
41. Chen AX, Zito W, Nash RA. Solubility enhancement of nucleosides and structurally related compounds by complex formation. Pharm Res. 1994;11(3):398–401.
42. Hussain MA, Diluccio RC, Maurin MB. Complexation of moricizine with nicotinamide and evaluation of the complexation constants by various methods. J Pharm Sci. 1993;82(1):77–9.
43. Suzuki H, Sunada H. Mechanistic studies on hydrotropic solubilization of nifedipine in nicotinamide solution. Chem Pharm Bull. 1998;46(1):125–30.
44. Beroi LM, Alexander KS, Riga AT. Study of interaction between ibuprofen and nicotinamide, using differential scanning calorimetry, spectroscopy, and microscopy and formulation of a fast-acting and possibly better ibuprofen suspension for osteoarthritis patients. J Pharm Sci. 2005;94(1):93–101.
45. Sanghvi R, Evans D, Yalkowsky SH. Stacking complexation by nicotinamide: a useful way of enhancing drug solubility. Int J Pharm. 2007;336(1):35–41.
46. Coffman RE, Kildsig DO. Effect of nicotinamide and urea on the solubility of riboflavin in various solvents. J Pharm Sic. 1996;85 (9):951–4.